ELSEVIER

Journal of Nuclear Materials 266–269 (1999) 969–974

journal of nuclear materials

Study of the radio-frequency driven sheath in the ion cyclotron slow wave antennas

T. Imai *, H. Sawada, Y. Uesugi [1], S. Takamura

Graduate School of Engineering, Center for Integrated Research in Science and Engineering, Nagoya University, Furo-cho, Chikusa-ku, Nagoya, 464-8603, Japan

Abstract

Formation of the radio-frequency driven sheath and resulting parasitic antenna loading in the ion cyclotron slow wave antennas are studied experimentally in the linear divertor plasma simulator NAGDIS-II. A phased loop antenna array with a poloidal mode of $m = 0$ is used in the present ICRF heating experiment. A large DC voltage drop of about several hundreds volts is induced on the loop antennas with and without Faraday screen during high power RF heating and causes the additional power dissipation (P_{sh}) due to the heat flux to the antenna current strap of ions accelerated by the RF driven DC sheath potential. This parasitic antenna loading is measured by calorimetric method and compared with that obtained from the conventional measurement of the antenna voltage and current. When a Faraday screen is employed to reduce the antenna–plasma interaction, P_{sh} becomes much smaller than the radiated RF power. The net antenna loading for ICRF slow wave excitation is evaluated, taking account of the RF sheath dissipation.

Keywords: Calorimetry; Heat flux; ICRF; Power balance

1. Introduction

Radio-frequency (RF) plasma heating in the ion cyclotron range of frequency (ICRF) has a promising auxiliary heating method for reactor plasmas because high power RF sources are commercially available and inexpensive compared with other plasma heating methods, and it has a good capability of core plasma heating and current drive. In contrast to these advantages, however, the ICRF heating has several problems related to the antenna–plasma interaction, such as antenna loading, impurity generation from the antenna structure and so on. The electrostatic Faraday screen (FS) is generally used to suppress the strong electrostatic interaction between the ICRF antenna and edge plasmas near the antenna. It is recognized that FS suppresses the electrostatic field parallel to the magnetic field ($E_{\|}$), and particle and heat fluxes into the antenna current strap effectively. Even with FS, however, impurity generation from FS is a severe problem in high power ICRF heating experiments [1,2]. Recent researches on the ICRF antenna-edge plasma interaction have shown that the RF driven sheath on the FS has a key role on the impurity generation form FS by ion sputtering [3–6]. The ion flow accelerated in the RF driven sheath causes an additional heat load on the antenna structure and gives a power loss in the RF system, transferring energy the RF field to the antenna material surface through the ion bombardment. In addition, the RF driven sheath may bias the edge plasma potential near the ICRF antenna and drive steady state convective cells in the scrape-off layer. These induced convective cells are possible to modify the particle and heat transport in the scrape-off layer [7,8].

So far, the effects of RF driven sheath on the ICRF antenna–plasma interaction are studied theoretically and analyzed using experimental data of high power ICRF heating in large tokamaks. During high power ICRF heating, direct measurements of RF driven sheath voltage of the powered antenna current strap and its FS, and the antenna heat load due to the accelerated ion flow have not been done. In the present experiment using a linear plasma device, both the DC and RF

* Corresponding author.
[1] E-mail: uesugi@nuee.nagoya-u.ac.jp.

0022-3115/99/$ – see front matter
PII: S0022-3115(98)00625-4

voltages on the antenna current strap and FS of the loop antenna for ICRF slow wave heating are measured and compared with theoretical estimation. Simultaneously the plasma heat load to the antenna current strap and FS is measured with calorimetry to obtain the additional RF power dissipation by the RF induced sheath. The net radiated RF power for the excitation of ICRF slow waves is estimated from the conventional RF power measurement and the antenna heat load.

2. RF driven sheath and antenna heat load

According to Ref. [6], the voltage driving the sheath is given by $V_{rf} = \int ds\, E_{\|}$, where $E_{\|}$ is the component of the RF electric field parallel to the magnetic field, and it is mainly induced by the mismatch of the FS elements with the magnetic field line. When sufficient density plasmas are present on field line segments intersecting the antenna structure, the electron moves to short out the electric field, leaving sheaths of positive space charge. A steady state DC potential V_0 (rf driven DC sheath) is produced by rectification of V_{rf} in the sheath, confining electrons and maintaining quasi-neutrality. In the parallel plate model of RF driven sheath this rectified DC potential is given by

$$\frac{eV_0}{T_e} = \chi_B + \ln[I_0(\xi)], \tag{1}$$

where $\xi = eV_{rf}/T_e$, $\chi_B = 0.5 \ln (m_i/2\pi Z m_e)$ and I_0 is a modified Bessel function. In large V_{rf} limit, $\xi \gg 1$ and the asymptotic value of V_0 is given by

$$eV_0 \sim eV_{rf} - (T_e/2)\ln(2\pi eV_{rf}/T_e) + \chi_B. \tag{2}$$

The power dissipation in the RF driven sheath (P_{sh}) is also calculated from V_{rf} and current flow into the antenna structure. The sheath power dissipation P_{sh} is given by

$$P_{sh} = A\langle\Gamma\rangle T_e \xi I_1(\xi)/I_0(\xi), \tag{3}$$

where $\langle\Gamma\rangle (= Zn_i c_s)$ is the time averaged particle flux into the antenna and A is a surface area of the antenna structure. For $\xi \gg 1$, P_{sh} is simplified to $P_{sh} \sim An_i c_s$ ($Ze V_{rf}$). As shown in Eq. (2) the large V_{rf} limit gives $V_0 \sim V_{rf}$, and the sheath power dissipation is simply dominated by the power delivered to the antenna by ions accelerated in the rectified potential $V_0 \sim V_{rf}$. Other heat flow into the antenna comes from the electron and ion heat flux from the presheath. The time averaged electron heat flux is given by

$$\langle H_e\rangle = \frac{n_e 2T_e v_e}{(2\pi)^{1/2}} \exp(-\chi_0) I_0(\xi), \tag{4}$$

where $\chi_0 = eV_0/T_e$, v_e is the electron thermal velocity. In the limit of small ξ both electron and ion contributions should be dominant.

The RF power dissipation given by Eq. (3) is an additional dissipated power for the RF heating system and also additional heat load to the antenna structure. The power coupled to the plasma through wave excitation P_{rf}, and the dissipated power in the RF driven sheath are independent loss channels driven by antenna current. In this case the antenna loading resistance R_L is given by

$$R_L = \frac{P_{rf} + P_{sh}}{I_{ant}^2}, \tag{5}$$

where I_{ant} is the antenna current. In Ref. [6] it is shown that P_{rf} and P_{sh} have different scalings like $P_{rf} \propto V_{ant}^2 \propto I_{ant}^2$ and $P_{sh} \propto V_{ant} \propto I_{ant}$, respectively. From these scalings the antenna loading resistance is dependent on the RF power. In high rf power limit, $P_{rf} \gg P_{sh}$, R_L becomes constant, and R_L scales as $1/\sqrt{P_{rf}}$ at low power level $P_{sh} > P_{rf}$. The conventional measurement of R_L can not separate the P_{sh} contribution from the antenna loading. In the present work the antenna heat load due to RF sheath dissipation is discriminated with calorimetric method and compared with the theoretical estimation shown above. The antenna voltage and particle flux into the antenna current strap and FS are also measured separately. From these observations the net antenna loading resistance shown by $R_L = P_{rf}/I_{ant}^2$ and the real coupling efficiency for ICRF slow wave excitation are obtained.

3. Experiment

RF heating experiments have been carried out in a linear divertor plasma simulator NAGDIS-II [9]. High density He plasmas up to 6×10^{19} m^{-3} can be generated in steady state. The static magnetic field can be operated up to 0.25 T. The ICRF slow wave heating is employed in NAGDIS-II since slow waves can be absorbed by electrons through Landau damping and strongly damped by ion cyclotron resonance [10]. By choosing the ratio of ω/ω_{ci}, the wave absorption by electrons and ions can be controlled. The RF system for ICRF slow wave heating is shown in Table 1. The ICRF slow waves are excited by phased 4 loop antennas located at the high field region of the magnetic beach configuration along

Table 1
Specification of SIT inverter RF power supply in NAGDIS-II

Power source	Static Induction Transistor (SIT)
Operating frequency	0.5–1.5 MHz
Output power	14 kW per unit in CW mode
	20 kW per unit in 1 s pulse
	4 units in operation
Phase control	$0 \sim 2\pi$
	5° step
Output impedance	<0.6 Ω

the magnetic field. Each loop antenna has 3 turn coil and single layer Faraday screen. The antenna current coil is made by copper tube and water-cooled. Both the antenna coil and FS are isolated from the vacuum chamber in order to avoid direct DC discharges between the hot cathode of NAGDIS-II plasma generator and antenna structure. A schematic diagram of one of the phased 4 loop antenna array is shown in Fig. 1. In the present experiment the magnetic field at the antenna section is kept at 0.23 T and the electron density at the column center is about 5×10^{18} m^{-3} and about 3×10^{17} m^{-3} near the antenna. The driving frequency is fixed at 780 kHz, where $\omega/\omega_{ci} = 0.91$ for singly ionized He ion.

3.1. Measurement of antenna voltage and heat load

The antenna voltages of current loop and FS with respect to the vacuum chamber, both RF amplitude and DC sheath voltage are measured through RF voltage dividers. Typical antenna voltage waveforms during RF heating are shown in Fig. 2 as a parameter of the antenna current. In the present antenna system RF voltage is applied between each end of the antenna current coil (balance feeding). The measured RF voltages are induced by the electrostatic coupling between the powered antenna, and FS and vacuum chamber. In Fig. 3 DC sheath voltage of the antenna current coil is shown as a function of the induced RF voltage (0 to peak voltage) on the antenna coil. The DC voltage in the figure is obtained by averaging RF voltages measured at each feeding point of the loop antenna. Both the RF amplitude and negative DC sheath voltage increases linearly with antenna current, which means that V_{rf} and V_0 is proportional to $\sqrt{P_{rf}}$. The electron temperature near the antenna during RF heating is about 3–5 eV, which gives $\xi = eV_{rf}/T_e \gg 1$ in our experimental condition. In this region Eq. (2) shows $V_0 \sim V_{rf}$, which agrees with the experimental results without FS shown in Fig. 3. On the other hand the DC sheath voltage with FS is $V_0 \sim 2V_{rf}$ much larger than that without FS. Since the antenna conductor with FS is surrounded by the FS elements and side guard limiters, the density is much smaller than that outside the FS, roughly two orders of magnitude lower. The simple sheath theory may not be applied to the analysis of RF driven sheath as described in Section 2. The induced RF and DC voltage of FS shown in Fig. 4 is much smaller than that of the antenna current coil because the RF electric field of the antenna near field parallel to the magnetic field is effectively shielded.

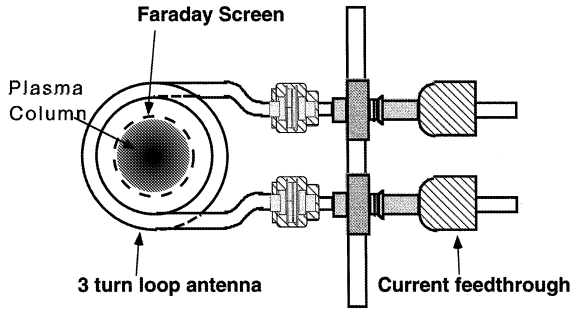

Fig. 1. Cross sectional view of 3 turn loop antenna. The antenna conductor is made of 9.53 mm copper tube and its diameter is 80 mm. The diameter of single layer Faraday screen is 50 mm. Both the antenna conductor and supporting structure of FS are water-cooled. The material of FS is molybdenum.

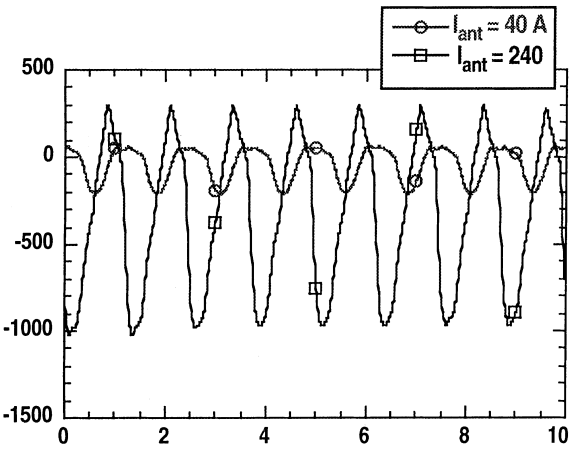

Fig. 2. Voltage waveform of the antenna current coil without Faraday screen. The driving frequency of the antenna is 780 kHz.

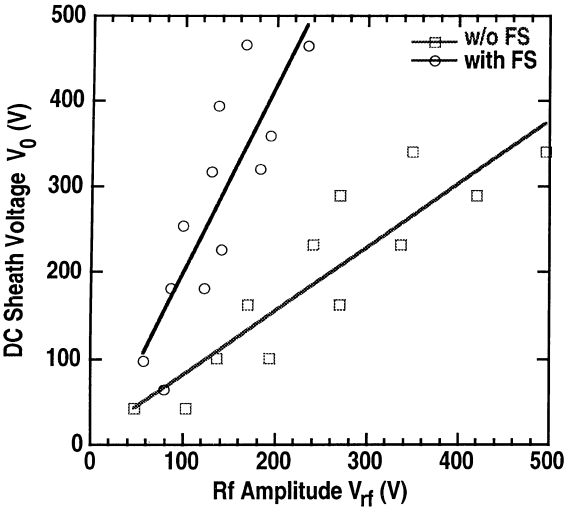

Fig. 3. RF driven DC sheath voltage as a function of RF voltage on the antenna current coil with and without FS. RF antenna current is changed from 40 to 250 A in this figure. The RF voltage shown in the figure is the amplitude from 0 to peak voltage.

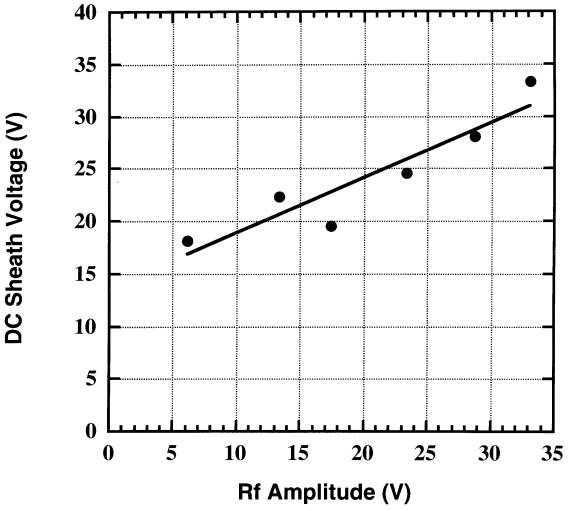

Fig. 4. RF driven DC sheath voltage of the Faraday screen as a function of the RF voltage induced on FS. The antenna current range is the same as that in Fig. 3.

The ion flux into the antenna coil and FS is directly measured or estimated from the plasma density and electron temperature near the antenna location, which are measured by fast scanning Langmuir probe. The heat loads to the antenna coil and FS measured by calorimetry are shown in Fig. 5 as a function of the antenna current. The plasma heat load shown in the figure is obtained from the difference of the heat load with and without RF input to the antenna. The experimental error of the present heat load measurement is estimated about ±30 W. Without FS the antenna heat load increases nearly in proportion to the antenna current. The antenna heat load without FS is compared with the theoretical estimation using Eq. (3) in Fig. 6. Theoretically estimated heat load is about 40% larger than the experimental value. This difference might be caused by the experimental errors for heat load measurement, and density and temperature measurement by Langmuir probes. The particle flux into the antenna coil is strongly suppressed by FS and consequently, the heat flow into the antenna coil with FS is much less than that without FS. The ion flux into the antenna coil with FS (Ion current ~50 mA) gives the estimated heat load of about 30–60 W at the maximum RF power, which agrees roughly with the experimental one. The heat load to FS is also measured during RF heating. The heat load to FS does not change significantly from that without RF. The RF sheath dissipation of FS is roughly estimated less than 20 W in the present experimental condition.

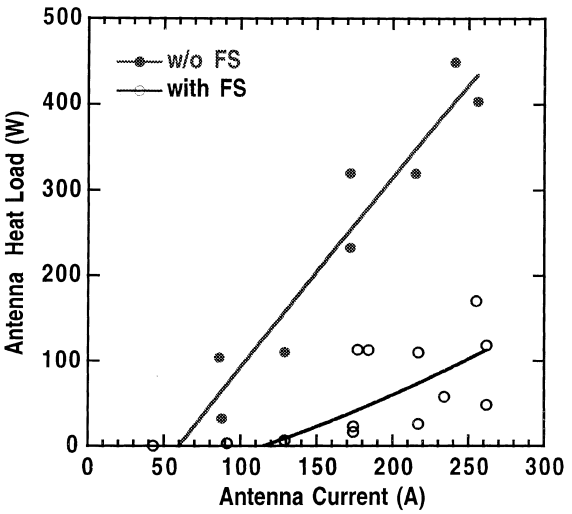

Fig. 5. Heat load to the antenna current coil as a function of the antenna current. The antenna heat load in the plasma is obtained from the difference between the heat load with and without plasma loading. In vacuum the antenna heat load is due to the Joule loss of the RF current flowing to the antenna conductor.

3.2. Estimation of the antenna loading

The antenna loading measurement shows that the vacuum loading resistance of the present RF antenna system is about 0.13 Ω and the plasma loading resistance given by Eq. (5) is 0.01–0.02 Ω at 780 kHz in the NAGDIS-II experimental condition. This low antenna loading resistance limits the heat load measurement at higher RF power range above 1 kW in the present RF heating system. As mentioned previously the conven-

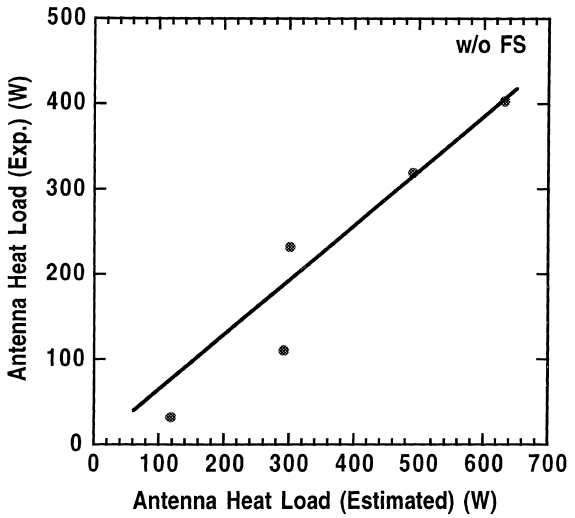

Fig. 6. Comparison of the experimentally observed antenna heat load with theoretical one in the case of the antenna without FS.

tional antenna loading measurement includes the loading due to RF sheath power dissipation. The net radiated RF power can be estimated by substracting the antenna heat load from the total RF power dissipation except for the RF circuit loss. The radiated power evaluated from the conventional measurements of RF voltage and current of the antenna and antenna heat load measured by calorimetry are shown in Fig. 7(a) and (b). Without FS the antenna heat load is much higher and almost comparable to the RF power. On the other hand the antenna heat load is much smaller than the RF power with FS. In the present experiment the measured

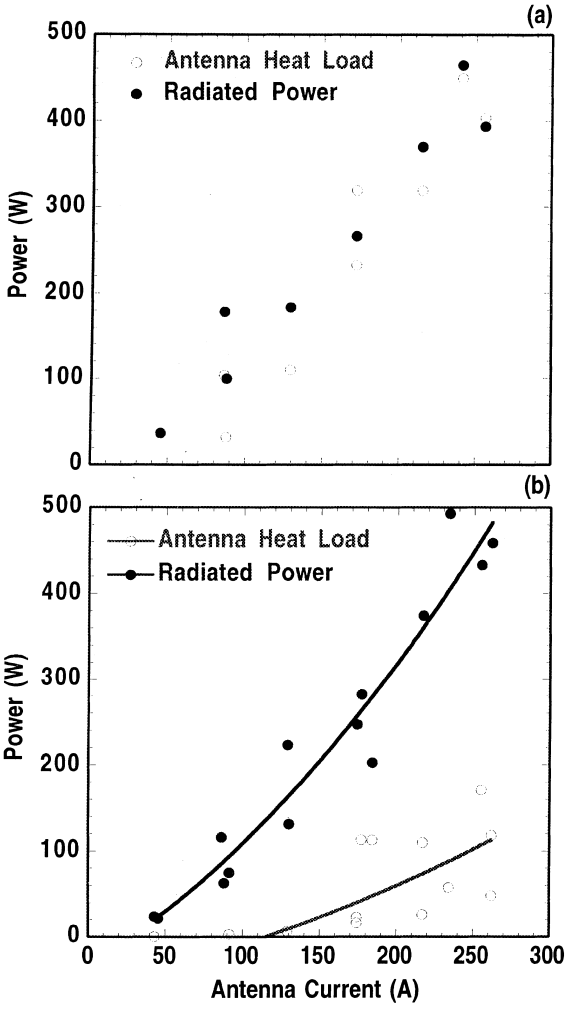

Fig. 7. Radiated RF power calculated from the antenna voltage and current of the loop antenna and the antenna [without FS (a) and with FS (b)] heat load measured by calorimetry as a function of the antenna current. The radiated RF power is calculated from the difference between the RF dissipation of the antenna system including the impedance matching circuit with and without plasma loading.

antenna heat load includes both the RF sheath dissipation and the electron and ion heat flow from the presheath. In high power region where $\xi = eV_{rf}/T_e \approx eV_0/T_e \gg 1$ for thermal electrons, the electron heat flow given by Eq. (4) can be neglected. The heat flow due to the energetic electrons and ions generated by excited slow waves is not clear so far. It can be concluded that the most of RF power is dissipated by RF driven sheath in the case of the antenna without FS. With FS the effective reduction of the RF sheath dissipation is obtained and 80% of the RF power is dissipated by radiation. The experimental observations show that the center electron temperature rises from 10 eV to ~12 eV by 500 W RF input with FS but it rises to ~11 eV in the case of without FS. In contrast with the center electron temperature the edge temperature near the antenna shows an opposite tendency that the edge temperature during RF heating without FS is 3.5–5 eV while that with FS is 2.5–3 eV. The RF power radiated from the antenna without FS might couple to the edge plasma near the antenna.

4. Summary

The RF amplitude and RF driven DC sheath voltage induced on the ICRF slow wave antenna are directly measured and compared with the theoretically estimated one using simple sheath theory. Even with FS high RF driven DC sheath voltage of about several hundreds volts is induced, which value is much larger than that expected from simple sheath theory. Without FS the antenna current coil directly touches the high density edge plasmas and induced DC sheath voltage agrees well with that of theoretical estimation. The antenna heat load measurement shows that the RF dissipation caused by the RF induced DC sheath is nearly comparable to the RF input power to the antenna. With FS the antenna heat load is greatly suppressed to about 20% of input RF power.

Acknowledgements

The authors are grateful to Dr N. Ohno for useful discussions about RF experiments in NAGDIS-II. And we also thank Mr T. Fusato for technical assistance on RF power source.

References

[1] EQUIPE TFR, Plasma Phys. 24 (1982) 615.
[2] H. Tamai, K. Odajima, H. Matsumoto, et al., Nucl. Fusion 26 (1986) 365.

[3] J.R. Myra, D.A. D'lppolito, M.J. Gerver, Nucl. Fusion 30 (1990) 845.
[4] R. Myra, D.A. D'lppoloto, M. Bures, Phys. Plasmas 1 (1994) 2890.
[5] T. Tanaka, R. Majesky, D.A. Diebold, N. Hershkowitz, Nucl. Fusion 36 (1996) 1609.
[6] D.A. D'lppoloto, J.R. Myra, Phys. Plasma 3 (1996) 420.
[7] D.A. D'lppoloto, J.R. Myra, Phys. Fluids B 5 (1993) 3603.
[8] R.H. Cohen, D.D. Ryutov, Nucl. Fusion 37 (1997) 621.
[9] N. Ezumi, N. Ohno, Y. Uesugi et al., in: Proceedings of the 24th EPS Conference on Controlled Fusion and Plasma Physics, Berchtesgarden, 1997, vol. 21A, part III, p. 1225.
[10] Y. Uesugi, S. Watanabe, S. Ohsawa, S. Takamura, et al., in: Proceedings of the 12th Topical Conference on Radio Frequency Power in Plasmas, Savannah, GA, 1997 p. 429; S. Watanabe, S. Ohsawa, M. Takagi, et al., in: Proceedings of the 12th Topical Conference on Radio Frequency Power in Plasmas, Savannah, GA, 1997 p. 483.